Accepted Manuscript

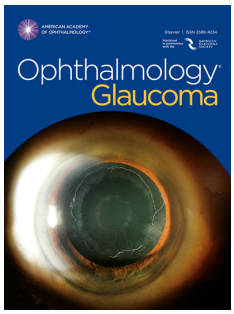

Haemoglobin Video Imaging provides novel in vivo high-resolution imaging and quantification of human aqueous outflow in glaucoma patients

Tasneem Z. Khatib, Paul AR. Meyer, Jed Lusthaus, Ilya Manyakin, Yusuf Mushtaq, Keith R. Martin

PII: S2589-4196(19)30063-8

DOI: https://doi.org/10.1016/j.ogla.2019.04.001

Reference: OGLA 83

To appear in: *OPHTHALMOLOGY GLAUCOMA*

Received Date: 17 December 2018

Revised Date: 14 March 2019

Accepted Date: 1 April 2019

Please cite this article as: Khatib TZ, Meyer PA, Lusthaus J, Manyakin I, Mushtaq Y, Martin KR, Haemoglobin Video Imaging provides novel in vivo high-resolution imaging and quantification of human aqueous outflow in glaucoma patients, *OPHTHALMOLOGY GLAUCOMA* (2019), doi: https://doi.org/10.1016/j.ogla.2019.04.001.

Title Page

Title: Haemoglobin Video Imaging provides novel in vivo high-resolution imaging and quantification of human aqueous outflow in glaucoma patients

Authors' full names and institutions:

Tasneem Z Khatib[1,2] Paul AR Meyer[2], Jed Lusthaus[2,3,4], Ilya Manyakin[5], Yusuf Mushtaq[6] and Keith R Martin[1,2,7,8]

1. John van Geest Centre for Brain Repair, University of Cambridge
2. Eye Department, Cambridge University Hospitals NHS Foundation Trust, Cambridge
3. Sydney Eye Hospital Glaucoma Unit, Sydney, Australia
4. Discipline of Ophthalmology, The University of Sydney, Australia
5. Department of Physics, University of Cambridge, UK
6. School of Clinical Medicine, University of Cambridge, Cambridge, UK
7. Cambridge NIHR Biomedical Research Centre
8. Wellcome Trust – MRC Cambridge Stem Cell Institute, University of Cambridge

Corresponding author: Keith Martin, 01223-216427 (tel), krgm2@cam.ac.uk, John van Geest Centre for Brain Repair, Forvie Site, Robinson Way, Cambridge CB2 0PY

Meeting Presentation: This material has been presented in part at the Association for Research in Vision and Ophthalmology Annual Meeting, 2017.

Grant information:

This work was supported by grants from Addenbrooke's Charitable Trust, the HB Allen Charitable Trust, the Cambridge Eye Trust, the Jukes Glaucoma Research Fund and a core support grant from the Wellcome Trust and MRC to the Wellcome Trust – Medical Research Council Cambridge Stem Cell Institute.

Conflict of Interest: No conflicting relationship exists for any author.

Running head: Human aqueous outflow imaging

This manuscript contains 5 video clips as additional online-only material

Abstract

Purpose: Non-invasive, detailed measurement of the dynamics of human aqueous outflow is difficult to achieve with currently available clinical tools. Here we used haemoglobin video imaging (HVI) to develop a technique to image and quantify human aqueous outflow non-invasively and in real time.

Design: A prospective observational study to describe characteristics of aqueous veins and a pilot prospective interventional feasibility study to develop quantification parameters.

Subjects, Participants, and/or Controls: Patients were recruited from the Addenbrooke's Hospital Glaucoma clinic. The observational study included 30 eyes and the pilot interventional feasibility study was performed on 8 eyes undergoing selective laser trabeculoplasty (SLT). Our SLT protocol also included the installation of pilocarpine and apraclonidine eye drops.

Methods, Intervention, or Testing: Participants underwent HVI alongside their usual clinic visit.

Main Outcome Measures: The change in cross sectional area (CSA) of the aqueous column (AQC) within episcleral veins was correlated with IOP reduction and change in visual field mean deviation before and after intervention. Fluctuations in contrast and pixel intensity of red blood cells in an aqueous vein were calculated to compare the flow rate before and after intervention using autocorrelation analysis.

Results: HVI enables the direct observation of aqueous flow into the vascular system. Aqueous is seen to centralise within a laminar venous

column. Flow is pulsatile, and fluctuations of flow through globe pressure or compression of the aqueous vein are observed.

There was a significant increase in the AQC following the administration of our SLT protocol (n=13; $p<0.05$). This correlated with the degree of IOP reduction (n=13; Pearson's correlation coefficient 0.7; $p=0.007$) and the improvement in mean deviation (MD) observed post intervention (n=8; Pearson's correlation coefficient 0.75; $p=0.03$). Autocorrelation analysis demonstrated a faster rate of decay in an aqueous vein following intervention indicating an increase in flow rate.

Conclusions: HVI can be incorporated into a routine clinic slit lamp examination to allow a detailed assessment and quantification of aqueous outflow in real time. It has the potential to be used to help target therapeutic interventions to improve aqueous outflow and further advance our understanding of aqueous outflow dysregulation in the pathogenesis of glaucoma.

Introduction

Non-invasive, detailed measurement of the dynamics of human aqueous outflow is difficult to achieve with currently available clinical tools. Our knowledge of the anatomy and physiology of aqueous outflow is based on studies in *ex vivo* tissue [1,2–4] as well as *in vivo* techniques that are either static,[5] invasive or involve a degree of manipulation of physiological parameters.[4] The widely used fluorescein disappearance test[6,7] is at best an indirect estimate of aqueous outflow and the outflow pathway cannot be visualised using this technique.

The advent of minimally invasive glaucoma surgery (MIGS) procedures has led to renewed interest in the dynamics of aqueous outflow. The intraocular pressure (IOP) lowering effect of trabecular bypass devices is variable in different patients. [8–12] The segmental and dynamic nature of aqueous outflow has previously been described[3,4] and it has been suggested that targeting trabecular bypass stents to ocular quadrants with good aqueous outflow could improve the success rates of these procedures.

Here we describe a technique to visualise aqueous veins non-invasively using haemoglobin video imaging[13] (HVI) which utilises the haemoglobin absorption spectrum to enhance the contrast between red blood cells and their surroundings. Erythrocytes are displayed as darker objects against a brighter background of light reflected by sclera with a resolution down to the level of a single red blood cell. Aqueous is observed as an erythrocyte void, a clear column which displaces red blood cells as it flows into the episcleral venous circulation.

We describe characteristics of aqueous veins that are consistent with earlier reports and we have developed a quantification technique to measure the cross sectional area (CSA) of the aqueous column within episcleral veins. As an example of the type of clinical investigation possible with our technique, we performed a pilot study on 8 eyes of 7 patients who underwent selective laser trabeculoplasty (SLT) together with administration of pilocarpine and apraclonidine eye drops, as per our standard protocol, and correlated the change in CSA with IOP reduction

and change in visual field mean deviation before and after intervention. We also propose a method that could be used to compare the flow rate from HVI images before and after intervention.

HVI can be incorporated into a routine clinic slit lamp examination to allow a detailed assessment of physiological and pathological aqueous outflow in real time. We suggest that HVI has the potential to be used as a tool to help target therapeutic interventions, to improve aqueous outflow and to further advance our understanding of aqueous outflow dysregulation in the pathogenesis of glaucoma.

Methods

The study was conducted in accordance with the tenets of the Declaration of Helsinki. The Institutional Review Board of Cambridge University Hospitals NHS Foundation Trust and the Local Research Ethics Committee approved the study (REC reference number: 15/LO/2171) . All subjects gave written informed consent before participation in the study.

Imaging aqueous veins in Human Eyes

We performed an observational study on 30 glaucomatous eyes to determine characteristics of aqueous veins using HVI. Images were captured using a monochromatic Prosilica GC1380H camera attached to a Zeiss SL130 slit lamp. As described previously,[13] the slit-lamp illumination system is fitted with a band-pass interference filter (steep long and short wavelength cut-off; >50% transmission between 505 and 575 nm) and a hot mirror that stops light with wavelengths beyond 730 nm from reaching the camera. The video camera is mounted on a 50% beam-splitter with a 220 mm focal length C-mount. Images are captured at 30 frames per second, without compression. During the live recording of aqueous veins, images are displayed in real time using bespoke HVI software.

Image processing

Raw image data was exported from the HVI software in .pgm format and processed using Image J. Image sequences were stabilised using the 'Image J Stabilizer' plugin (Video clips 1 and 2) prior to quantification. We

developed a computer model, demonstrating the changes in transmitted light along an orthogonal transept of a vein containing a central aqueous column. The diameter of the column was found to be the distance (δ) between intensity minima. For calculation of the cross-sectional area, we assumed the vessel had a circular section. Measurements were made upstream of a vessel confluence. We assessed the repeatability of measurements by comparing values from 4-10 separate images per eye for 9 individuals. For extended length sequences to enable detailed observation of aqueous vein characteristics, stabilisation was performed using Adobe After Effects CC (version 15.1.12).

Aqueous column cross-sectional area following our SLT protocol

We performed HVI on 8 eyes, immediately before and 10 minutes after selective laser trabeculoplasty (SLT). SLT energy settings were 0.3-1.2 mJ targeting 90-360^{o} of the trabecular meshwork. IOP was measured immediately before and 30 minutes post-procedure. Pilocarpine nitrate 2% (Bausch and Lomb) and apraclonidine 1% (Alcon) eye drops were instilled

30 minutes prior to SLT. The CSA of the aqueous column was calculated and correlated with the degree of IOP reduction observed and the change in mean deviation (MD) using 24-2 Humphrey visual field SITA standard testing pre and post intervention. The mean length of time for MD measurement post intervention was 23 weeks (range 15-30 weeks).

Quantifying flow rate

Aqueous flows as a central stream through a column of venous blood. Therefore, enhancement of aqueous drainage can be expected to increase the flow rate of the surrounding red blood cells and it is this effect that we aimed to exploit.

We used principles derived from photon correlation spectroscopy and laser doppler velocimetry where fluctuations in the recorded intensity signal are examined to estimate parameters such as particle size or velocity. For aqueous flow using successive HVI images, fluctuations in contrast and pixel intensity of red blood cells through an aqueous vein were calculated and used to compare the rate of flow before and after our SLT protocol.

Quantifying flow rate: fluctuation transformation

The sum of the absolute values of pixel-wise differences from successive stabilised HVI frames were taken:

$$d_{ij} = \sum_{t=0}^{N-1} |p_{ij}(t+1) - p_{ij}(t)|$$

where t denotes frame number, (i,j) denotes pixel coordinates of the individual pixels and $p_{ij}(t)$ is the pixel intensity in frame t, with N being the total number of recorded frames and d_{ij} being the un-normalised fluctuation value. In order to extract the relative scale of the fluctuations in comparison with the whole image, we then normalise the computed values as follows:

$$n_{ij} = (d_{ij} - \mu)/\sigma$$

where μ, σ are, respectively, the mean and standard deviations of the fluctuations values d_{ij} in the image. The results of the above

transformation before and after the intervention are illustrated in supplementary figure 1.

Quantifying flow rate: autocorrelation analysis

The above transformation was used to segment the pixels of interest from the background and compute an "autocorrelation" to quantify the timescale of pixel fluctuations and how fast the pixel values change. Pixels with normalized fluctuation value above a given threshold of 2.5 were selected and the mask applied to all frames in the video.

$$R_{ij}(n) = \frac{\mathbb{E}[\,(p_{ij}(t) - \mu)(p_{ij}(t+n) - \mu)]}{\sigma^2}$$

Where $R_{ij}(n)$ denotes the autocorrelation function value for a pixel at position (i,j) at a frame delay value *t*, μ is the mean pixel value in the segmented image, σ is the standard deviation of the pixel values in the segment. The mean signal was computed by averaging the autocorrelation across all pixels. In order to show invariance we also computed the autocorrelations for the background of the HVI images.

Results

The HVI technique demonstrates aqueous as an erythrocyte void at high contrast to haemoglobin in episcleral venous blood (Figure 1).

In every vein observed, aqueous centralised within a laminar venous column, regardless of its point of entry into the episcleral circulation (Figure 2; Video clip 3). A "∗" symbol briefly appears to denote the vessel(s) of interest in each video within the clip before disappearing to permit uninterrupted observation of flow dynamics. A corresponding header also identifies the main observation to be made from individual recordings.

The length and diameter of aqueous streams varied, but some continued beyond the conjunctival reflection. Fluctuations arose in the aqueous stream, corresponding with cardiac rhythm, eye movements and pressure on the globe (Figure 3, Video clip 4). Compression of the aqueous vein resulted in the redirection of aqueous flow to other vessels that had previously been filled with blood (Figure 4, Video clip 4).

The cross-sectional area calculations arising from δ (Figure 5) were consistent and repeatable for each eye measured. Any variation between repeated measurements did not correlate with the size of δ.

There was a significant increase in the AQC immediately following administration of our SLT protocol (Figure 6A) and this correlated with the degree of IOP reduction observed (Figure 6B) as well as the improvement in mean deviation (MD) observed post intervention (Figure 6C). Video clip 5 demonstrates individual aqueous veins from 4 glaucoma patients before and after intervention. Figure 7 uses example 1 (Video clip 5) to compute an autocorrelation analysis as described above and using the transformation and segmentation demonstrated in supplementary figures 1 and 2. There is an increase in the rate of decay following intervention indicating an increase in flow rate.

Discussion

We have used haemoglobin video imaging (HVI) to develop a method for the detailed observation and quantification of aqueous columns in

episcleral venous blood. This technique can be performed non-invasively as part of a routine clinic assessment using a modified slit lamp and repeated multiple times facilitating longitudinal examination of individual patients over a period of time. We confirm previous observations on the characteristics of aqueous flow, including laminar flow, pulsatility and altered dynamics corresponding to transient fluctuations in pressure, including the redistribution of aqueous following occlusion of an aqueous vein. We also propose a technique to compare flow rates in an aqueous vein using HVI images. The method is based on principles used in photon correlation spectroscopy and laser doppler velocimetry where the velocity of fluids in channels is calculated by measuring fluctuations in the recorded intensity signal. When tracer particles cannot be added to maintain the physiological parameters and monitor aqueous flow non-invasively, flow velocity estimation becomes more complex. We do not aim to provide a velocity estimate, as an accurate measurement of the decay rate would require a faster sampling rate and thus a faster frame rate

246 camera. However, the plots derived from autocorrelation analysis may be
247 useful as simple metrics for comparing flow in videos.

248 The ability to visualise and quantify physiological aqueous flow provides us
249 with the means to further explore the relationship between aqueous
250 outflow and the diagnosis, monitoring and treatment of glaucoma patients.
251 The correlation we have observed between well-established glaucoma
252 parameters such as intraocular pressure and mean deviation reinforces the
253 use of the aqueous cross-sectional area as a tool to quantify the outflow
254 status of an eye.

255 Our measurements using the SLT protocol were taken serially on the same
256 individual within an hour of each other immediately before and after
257 intervention. This enabled a direct assessment of the effects of SLT (with
258 simultaneous administration of apraclonidine and pilocarpine) on aqueous
259 outflow, irrespective of the known variations in outflow in a given
260 individual during a 24 hour period. While we have been able to quantify a
261 change in aqueous flow following intervention, the addition of pilocarpine

and apraclonidine as part of our protocol may also have affected aqueous flow and we cannot fully attribute our observed changes to SLT alone.

Establishing the variation in outflow in a healthy population is also essential prior to considering the use of aqueous outflow facility to assess and monitor glaucoma patients alongside intraocular pressure and mean deviation.

The ability to perform a dynamic assessment at high resolution while visualising aqueous and blood in real time may help to further our understanding of the relationship between episcleral venous pressure and aqueous flow. Current tools to measure episcleral venous pressure are at best limited. Modelling the redistribution of aqueous in the presence of raised episcleral venous pressure and the turbulence at the interface between aqueous and blood using HVI may provide an estimate of the pressure in the venous circulation and should be a focus of future work in this area.

The HVI technique could be used more readily as described here during the management of those patients where MIGS implantation is being considered. A more precise targeting of the site of implantation, to correspond with the anatomy of an individual's aqueous vein distribution, may improve the reliability of these devices in lowering intraocular pressure. The quantification of the aqueous column could also be used to assess the relative effectiveness of various MIGS devices as we have demonstrated here for SLT. This may facilitate refinement and stratification of the choice of MIGS according to the subset of patients most likely to benefit from a particular device.

References

1. Ashton N, Smith R. Anatomical study of Schlemm's canal and aqueous veins by means of Neoprene casts: III. Arterial relations of Schlemm's canal. *Br J Ophthalmol*. 1953;37(10):577-586.

2. Johnstone MA. The aqueous outflow system as a mechanical pump: Evidence from examination of tissue and aqueous movement in human and non-human primates. *J Glaucoma*. 2004;13(5):421-438.

3. Huang AS, Li M, Yang D, Wang H, Wang N, Weinreb RN. Aqueous Angiography in Living Nonhuman Primates Shows Segmental, Pulsatile, and Dynamic Angiographic Aqueous Humor Outflow. *Ophthalmology*. 2017;124(6):793-803.

4. Huang AS, Camp A, Xu BY, Penteado RC, Weinreb RN. Aqueous Angiography: Aqueous Humor Outflow Imaging in Live Human Subjects. *Ophthalmology*. 2017;124(8):1249-1251.

5. Kagemann L, Wollstein G, Ishikawa H, et al. Visualization of the conventional outflow pathway in the living human eye. *Ophthalmology*. 2012;119(8):1563-1568.

6. Jones RF, Maurice DM. New methods of measuring the rate of aqueous flow in man with fluorescein. *Exp Eye Res*. 1966;5(3):208-220. doi:10.1016/S0014-4835(66)80009-X.

7. Yablonski ME, Zimmerman TJ, Waltman SR, Becker B. A fluorophotometric study of the effect of topical timolol on aqueous humor dynamics. *Exp Eye Res*. 1978;27(2):135-142.

8. Shah M, Campos-Möller X, Werner L, Mamalis N, Ahmed IIK. *Midterm Failure of Combined Phacoemulsification with Trabecular Microbypass Stenting: Clinicopathological Analysis*. Vol 44.; 2018. doi:10.1016/j.jcrs.2018.03.030.

9. García-Feijoo J, Rau M, Grisanti S, et al. Supraciliary Micro-stent Implantation for Open-Angle Glaucoma Failing Topical Therapy: 1-Year Results of a Multicenter Study. *Am J Ophthalmol*. 2015;159(6):1075-1081.e1.

10. Samuelson TW, Katz LJ, Wells JM, Duh Y-J, Giamporcaro JE. Randomized Evaluation of the Trabecular Micro-Bypass Stent with Phacoemulsification in Patients with Glaucoma and Cataract. *Ophthalmology*. 2011;118(3):459-467.

11. Craven ER, Katz LJ, Wells JM, Giamporcaro JE. Cataract surgery with trabecular micro-

bypass stent implantation in patients with mild-to-moderate open-angle glaucoma and cataract: Two-year follow-up. *J Cataract Refract Surg*. 2012;38(8):1339-1345.

12. D. M, S. M, L. D, et al. Trabectome (trabeculectomy - internal approach): Additional experience and extended follow-up. *Trans Am Ophthalmol Soc*. 2008;106:149-159.

13. Meyer PAR. Re-orchestration of blood flow by micro-circulations. *Eye*. 2018;32(2):222-229.

Figure legends

Figure 1: Aqueous vein (arrow) captured using conventional techniques (A and B) and haemoglobin video imaging (C).

Figure 2: Examples of aqueous veins obtained using HVI (white arrows). Aqueous is seen as a centralised erythrocyte void.

Figure 3: Displacement of aqueous following digital pressure on the inferior globe. **A:** Aqueous vein (black arrow) prior to digital manipulation. **B-C:** Aqueous is redirected into an episcleral blood filled vessel following digital

pressure on the globe (white arrow). **D:** Immediate resumption of usual aqueous and blood flow following release of pressure.

Figure 4: Compression of an aqueous vein (white arrow) using a 10/0 vicryl loop redirects aqueous to a nearby episcleral blood vessel (black arrow).

Figure 5: A: Schematic representation of the intensity profiles of transmitted light in an aqueous vein using HVI **B-C**: Aqueous vein transept with corresponding density profile and δ measurement. Scale bar = 0.5 mm. **D:** Bland-Altman plot of the difference in paired δ measurements using HVI against the mean δ measurement.

Figure 6: AQC as a tool for quantifying aqueous outflow. A: Fold change in AQC cross-sectional area following intervention (n=13; $p<0.05$; Students ratio paired t-test). B: Correlation between IOP reduction and AQC CSA following intervention (n=13; Pearson's correlation coefficient 0.7; $p=0.007$)

C: Correlation between change in mean deviation and AQC CSA following intervention (n=8; Pearson's correlation coefficient 0.75; p=0.03)

Figure 7: Flow rate using autocorrelation analysis before and after SLT: A: Faster rate of decay is seen post intervention indicating an increase in flow rate. B: Similar autocorrelation decay rates seen in non-aqueous vein or background areas of the HVI images.

Supplementary figure 1: (Top) Pre intervention image (Bottom) Post intervention image. Notice the relative intensity increase of the treated vessel – the contrast of the vessel relative to the background is enhanced in comparison to the original by approximately one standard deviation.

Supplementary figure 2: Example of segmented images for blood flow in an aqueous vein before intervention (top) and after intervention (bottom).

371

372

373

374

375 **Video clip legends**

376 *Viewing order as in the text and in ascending order as numbered.*

377

378 **Video clip 1: unstabilised.mpg:** Captured images of an aqueous vein as

379 played back prior to stabilisation.

380

381 **Video clip 2: stablised.mpg:** Images as in video clip 1 following

382 stabilisation using Image J 'Image Stabilizer plugin'.

383

384 **Video clip 3: aqueous vein examples.mpg:** separate recordings of

385 individual aqueous veins using haemoglobin video imaging.

386

387 **Video clip 4: pulsatile.mpg:** Pulsatile nature of aqueous flow captured

using haemoglobin video imaging. 3 separate examples of displacement of aqueous following digital pressure on the globe away from the vessels of interest. Aqueous is redirected into an episcleral blood filled vessel following digital pressure on the globe with immediate resumption of usual aqueous and blood flow following release of pressure. A final example demonstrates compression of an aqueous vein using a 10/0 vicryl loop redirects aqueous to a nearby episcleral blood vessel. Aqueous flow resumes once the manoeuvre is complete.

Video clip 5: pre and post intervention.mpg: Imaging of individual aqueous veins in 4 glaucoma patients before and after intervention.

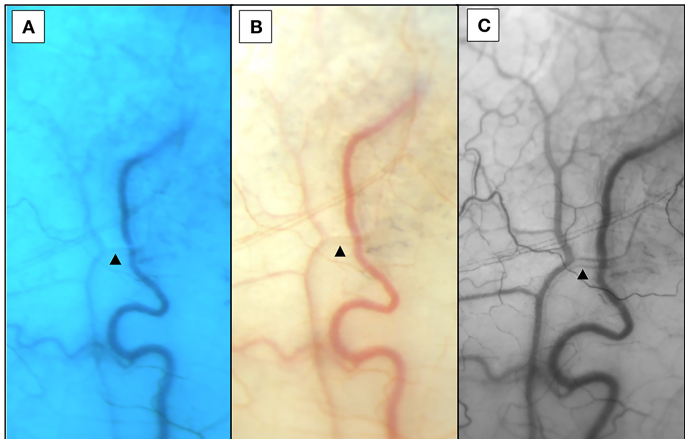

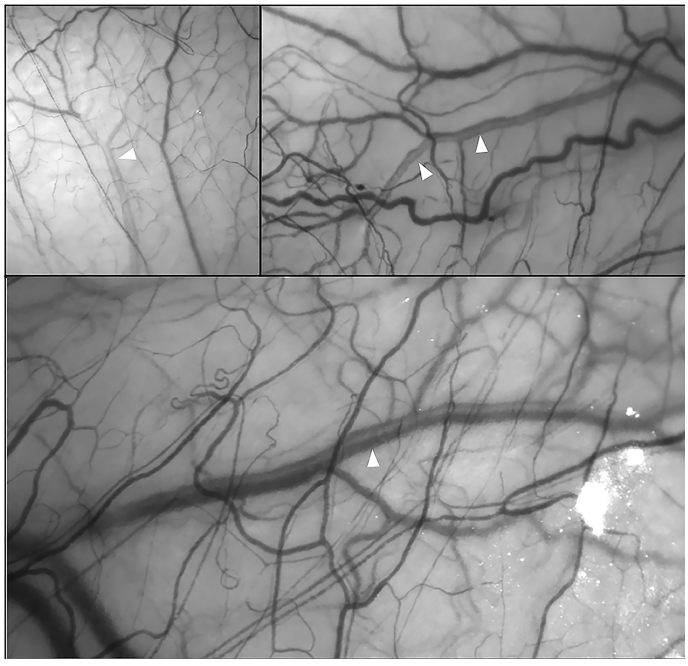

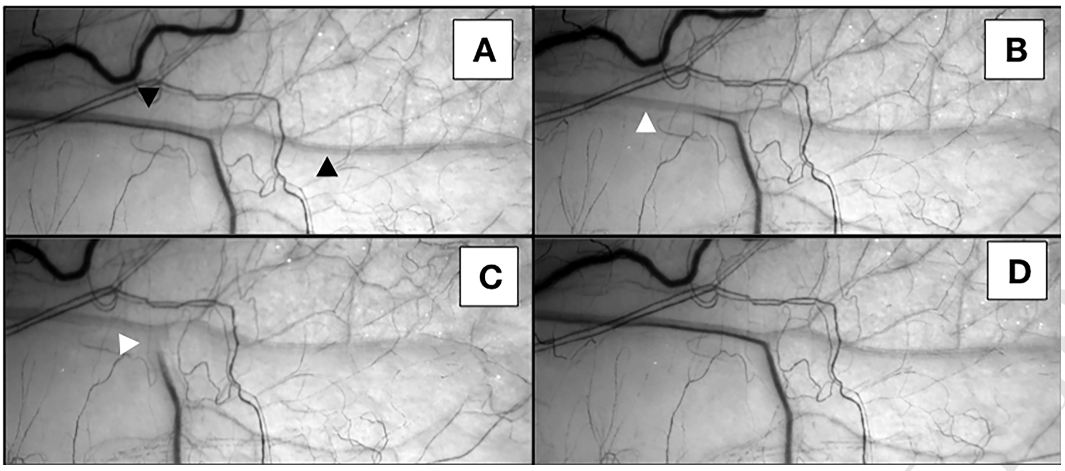

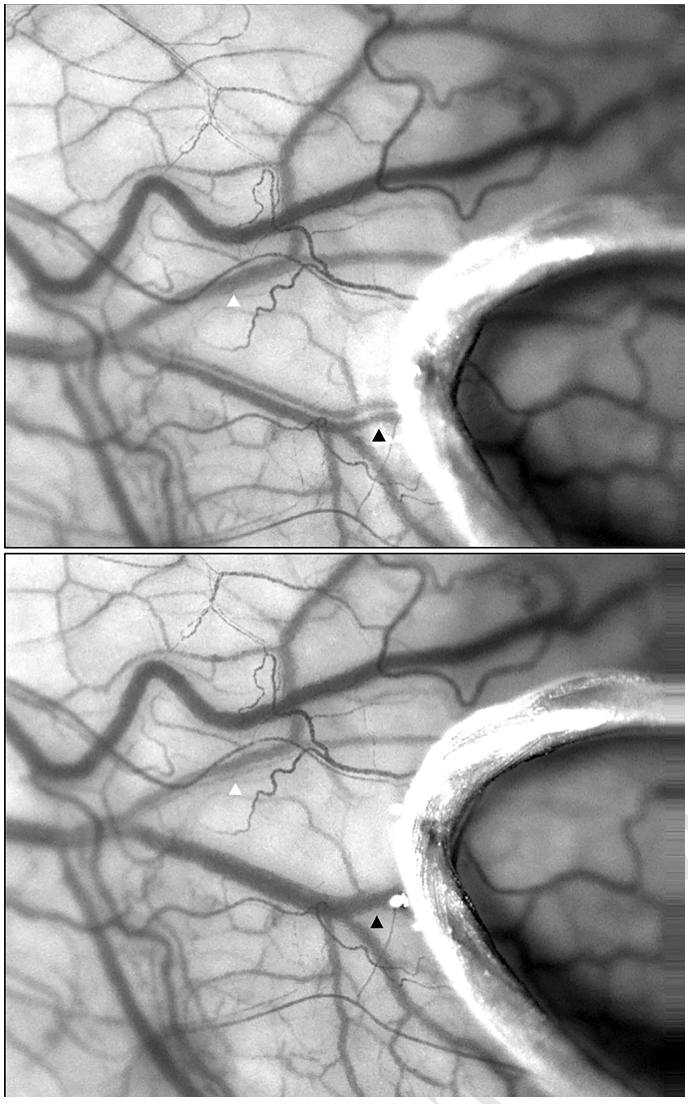

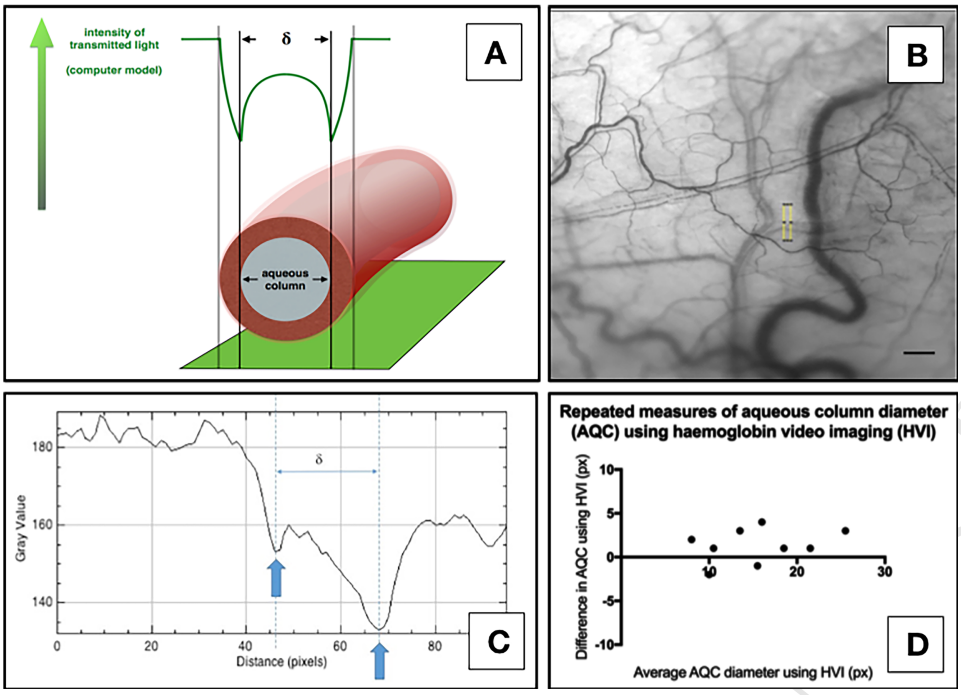

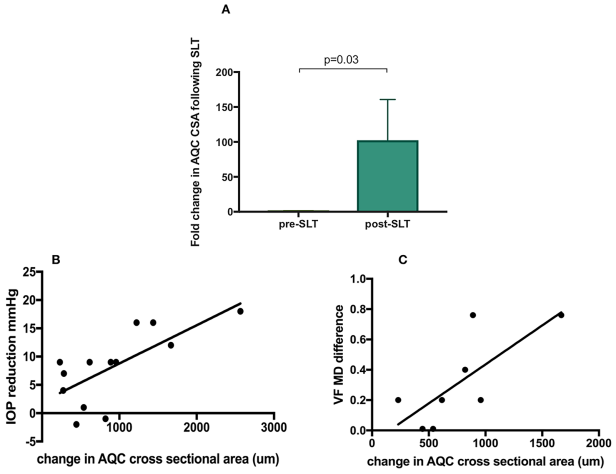

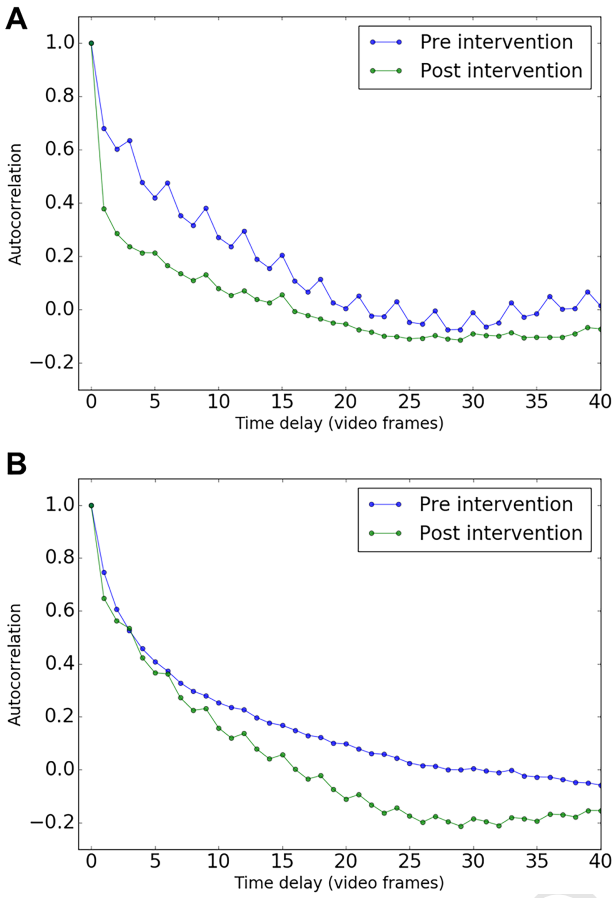

Précis

This study describes a technique to perform a detailed assessment and quantification of physiological and pathological aqueous outflow in real time and can be incorporated into a routine slit lamp examination in the clinic.